Journal of
Applied Crystallography
ISSN 0021-8898
Editor: **Anke R. Kaysser-Pyzalla**

The effect of gravity on the Debye–Scherrer ring in small-angle neutron scattering

D. F. R. Mildner and R. Cubitt

J. Appl. Cryst. (2012). **45**, 124–126

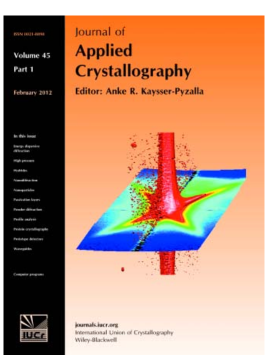

Journal of
Applied
Crystallography
ISSN 0021-8898

Received 16 November 2011
Accepted 9 January 2012

The effect of gravity on the Debye–Scherrer ring in small-angle neutron scattering

D. F. R. Mildner[a]* and R. Cubitt[b]

[a]Center for Neutron Research, National Institute of Standards and Technology, Gaithersburg, MD 20899, USA, and [b]Institut Laue–Langevin, 156X Centre de Tri, 38042 Grenoble, France. Correspondence e-mail: david.mildner@nist.gov

Gravity distorts the circular contours found for small-angle neutron scattering data from azimuthally symmetric scattering systems when taken at long wavelength and with large wavelength spreads. The resolution is calculated for a Debye–Scherrer ring and compared with results from measurements taken on a sample of opal.

1. Introduction

The pinhole geometry for small-angle neutron scattering measurements at the lowest values of scattering vector requires a long secondary flight path and a long-wavelength beam. Since neutrons are particles of mass m, the beam follows a parabolic trajectory on account of gravity. At the detector the beam has fallen, relative to the spectrometer axis defined by the source and sample apertures, by an amount that varies with the square of the neutron wavelength λ. The incident beam has some breadth of wavelengths so that azimuthally symmetric data are distorted at the smallest scattering angles. For randomly oriented samples the iso-intensity contours are no longer circular but oval on account of the extra gravitational contribution to the resolution. Corrections to the resolution for azimuthally averaged data as a function of scattering vector have been made relative to the spectrometer axis (Boothroyd, 1989) or to the beam center of the mean wavelength (Barker & Pedersen, 1995). Here we evaluate quantitatively the resolution width of a Debye–Scherrer ring as a function of azimuthal angle, showing how the wavelength and gravitational contributions are summed, and compare the results with measurements on opal.

2. Scattering vector variance

The scattered intensity is measured as a function of the magnitude of the scattering vector given by $Q = |\mathbf{Q}| = (4\pi/\lambda)\sin(\theta/2)$, where θ is the angle through which the neutron is scattered. At small scattering angles the scattering vector may be written $Q = k\theta$, where k $(= 2\pi/\lambda)$ is the neutron wavenumber. This gives rise to Debye–Scherrer rings of constant Q. Whereas the secondary path length and the mean wavelength determine the position of the scattering on the detector, the resolution or uncertainty in the measurement of Q also involves the collimation and the wavelength spread, and is given by

$$\sigma_Q^2 = k^2\sigma_\theta^2 + (Q/k)^2\sigma_k^2 = (2\pi/\lambda)^2\sigma_\theta^2 + Q^2(\sigma_\lambda/\lambda)^2. \quad (1)$$

The first term depends on the angular resolution, independent of both the direction and the magnitude of $\mathbf{Q}$, and is determined by the collimation and beam geometry of the spectrometer. The angular contribution to the variance of the scattering vector for pinhole geometry is given (Mildner & Carpenter, 1984) by

$$\begin{aligned}\sigma_{\rm geom}^2 &= k^2\sigma_\theta^2 \\ &= k^2\big[(1/4)(R_1/L_1)^2 + (1/4)(R_2/L')^2 + (1/12)(\Delta d/L_2)^2\big], \quad (2)\end{aligned}$$

where L_1 and L_2 are the incident and scattered flight paths, respectively, and $1/L' = 1/L_1 + 1/L_2$. R_1 and R_2 are the radii of the source and sample apertures, and Δd is the detector pixel width.

The second term represents the dispersion caused by the wavelength spread of the incident radiation and varies directly with the magnitude of $\mathbf{Q}$. The wavelength contribution to the variance of the scattering vector is given by

$$\sigma_{\rm wave}^2 = Q^2(\sigma_\lambda/\lambda)^2 = (kR/L_2)^2(\sigma_\lambda/\lambda)^2, \quad (3)$$

where the scattering angle $\theta = R/L_2$ and R is the distance of the detector element from the spectrometer axis. Often the incoming wavelength distribution is a triangular function with a mean wavelength λ_0, so that $(\sigma_\lambda/\lambda)^2 = (1/6)(\Delta\lambda/\lambda_0)^2$.

At the lowest values of scattering vectors there can be a significant extra gravitational contribution to the resolution. Simple kinetics shows that the change $\Delta y_{\rm g}$ in the vertical height of the beam of neutrons of wavelength λ at the detector is given by

$$\Delta y_{\rm g} = -L_2(L_1 + L_2)(g/2)(m/h)^2\lambda^2 = -A\lambda^2, \quad (4)$$

where g = 9.81 m s^{-2}, h is Planck's constant and $h/m = v\lambda$ = 3956 Å m s^{-1}, with v the neutron velocity. Therefore scattering vectors must be determined relative to the displaced beam center of the mean wavelength. Furthermore, the spread $\Delta\lambda$ in the wavelength results in a spread $2A\lambda(\Delta\lambda)$ in the vertical direction around that mean position. Consequently the effect of gravity introduces a third term, the gravitational contribution to the variance of the scattering vector, given by

$$\sigma_{\rm grav}^2 = (2A\lambda^2)^2(k/L_2)^2(\sigma_\lambda/\lambda)^2 \quad (5)$$

in the vertical direction only. This applies both to the incident beam and to neutrons scattered through small angles.

The components $\sigma_{\rm wave}$ and $\sigma_{\rm grav}$ are not independent; both depend on the wavelength resolution (σ_λ/λ) and therefore must first be summed in the direction of $\mathbf{Q}$ before the addition in quadrature with $\sigma_{\rm geom}$. Note that $\sigma_{\rm wave}$ is always in the direction of $\mathbf{Q}$, whereas only the component $-\sigma_{\rm grav}\sin\varphi$ is in the direction of $\mathbf{Q}$, where φ is the azimuthal angle of $\mathbf{Q}$ relative to the horizontal, that is,

$$\begin{aligned}\sigma_Q^2 &= \sigma_{\rm geom}^2 + (\sigma_{\rm wave} - \sigma_{\rm grav}\sin\varphi)^2 \quad \text{or} \\ \sigma_Q^2 &= \sigma_{\rm geom}^2 + \big[Q - 2A\lambda^2(k/L_2)\sin\varphi\big]^2(\sigma_\lambda/\lambda)^2. \end{aligned} \quad (6)$$

This equation shows how the width of a diffraction peak varies with azimuthal angle. It also applies to the incident beam at the detector for which $\mathbf{Q} = 0$.

3. Comparison with measurement

We apply this result to a neutron small-angle scattering measurement on opal, a silica–water system of closest-packed noncrystalline silica spheres of approximately 2000 Å in diameter. Opal gives a powder diffraction pattern at low scattering vectors, with the 111 and 220 Bragg reflections from the face-centered cubic lattice of these amorphous silica spheres (Graetsch & Ibel, 1997; Sosnowska & Shiojiri, 1999). Fig. 1 shows the scattering pattern taken on the D11 spectrometer (Lindner & Schweins, 2010) at a wavelength $\lambda_0 = 10$ Å, displaying the oval shape of the diffraction ring and the narrow resolution at the top ($\varphi = \pi/2$) compared to the larger width at the bottom ($\varphi = 3\pi/2$). The diffraction shows some degree of texture. Also shown is the faint second-order diffraction ring.

We first analyze the incident beam spot ($\mathbf{Q} = 0$). The path lengths used for the measurements are $L_1 = 40.5$ m and $L_2 = 39$ m, so that $A = 0.972$ mm Å^{-2}. Consequently the drop of the beam at the detector is $\Delta y_g = -97.2$ mm (or 12.96 pixels for $\Delta d = 7.5$ mm). The radii of the two apertures are $R_1 = 5$ mm and $R_2 = 4$ mm, so the spatial variance in the horizontal direction is $\sigma_x^2 = \sigma_r^2 = 25.90$ mm^2. The incident beam has a triangular wavelength distribution, which may be described by a Gaussian with an FWHM given by $\Delta\lambda/\lambda = 10\%$, so that $(\sigma_\lambda/\lambda)^2 = 0.18(\Delta\lambda/\lambda)^2$. The extra spatial variance in the vertical direction is $\sigma_g^2 = [2A\lambda^2(\sigma_\lambda/\lambda)]^2 = 68.14$ mm^2, so that $\sigma_y^2 = \sigma_r^2 + \sigma_g^2 = 94.03$ mm^2. These values give beam spot dimensions of $\Delta Q_x \times \Delta Q_y = (1.93 \times 3.68) \times 10^{-4}$ Å^{-1}, which are comparable to the measured values of $[2.06\ (2) \times 3.68\ (2)] \times 10^{-4}$ Å^{-1}.

We now consider the position of the diffraction ring relative to the beam center defined by the mean wavelength λ_0. The magnitude of the scattering vector at $\varphi = \pm\pi/2$ is $Q = Q_0 \mp (2\pi/L_2)A\lambda_0(\sigma_\lambda/\lambda)^2$. The difference between the two, 5.6×10^{-6} Å^{-1}, is an order of magnitude smaller than that found experimentally (see Table 1). However, regardless of any error in the determination of the beam center, the mean value of Q_0 is $3.83\ (2) \times 10^{-3}$ Å^{-1}. Also the mean magnitude of the scattering vector at $\varphi = 0$ and π, averaged over the wavelength spectrum, will be less than Q_0. Hence under gravity the circular ring becomes oval, flattened at the top and elongated at the bottom, with a narrower width in the horizontal. At larger scattering vectors such a ring becomes more circular, as observed in the second-order ring.

Table 1
Values of the measured and calculated width ΔQ (FWHM) for the Debye–Scherrer ring for opal shown in Fig. 1.

Azimuth φ	Measurement $\langle Q \rangle$ (10^{-3} Å^{-1})	Variance σ_Q^2† (10^{-8} Å^{-2})	Calculated ΔQ† (10^{-4} Å^{-1})	Measurement ΔQ† (10^{-4} Å^{-1})
0	3.76 (1)	3.33	4.30	5.4 (2)
$\pi/2$	3.81 (1)	0.77	2.06	3.5 (2)
π	3.78 (1)	3.33	4.30	4.7 (2)
$3\pi/2$	3.85 (2)	9.37	7.21	8.6 (4)

† Averaged over a $\Delta\varphi = 20°$ sector.

Finally we determine the width of the diffraction ring that occurs at a scattering vector $Q = 3.83 \times 10^{-3}$ Å^{-1} for opal. We find that the magnitudes of the three contributions to the variance of the scattering vector are comparable: $\sigma_{\rm geom}^2 = 6.71 \times 10^{-9}$ Å^{-2}, $\sigma_{\rm wave}^2 = 2.65 \times 10^{-8}$ Å^{-2} and $\sigma_{\rm grav}^2 = 1.77 \times 10^{-8}$ Å^{-2}. Using equation (6) we calculate the width of the diffraction ring as a function of azimuth φ, assuming Gaussian fits. The width of the ring for $\varphi = 3\pi/2$ is greater than that for $\varphi = \pi/2$. The longer wavelengths, relative to the shorter wavelengths, fall more at the bottom of the diffraction ring than at the top, such that the distribution is less concentrated at the bottom. In practice the measurements were computed over a 20° sector, so that the calculations also include similar averages over the azimuth. Table 1 shows the measured and calculated widths at different azimuths. (We observe that, for this spectrometer geometry and $\lambda = 10$ Å, the width at $\varphi = \pi/2$ is narrowest at $Q = 3.13 \times 10^{-3}$ Å^{-1} for which $\sigma_{\rm wave} = \sigma_{\rm grav}$. Conversely, the diffraction width for opal is narrowest at the top for $\lambda = 12.2$ Å with the same wavelength reso-

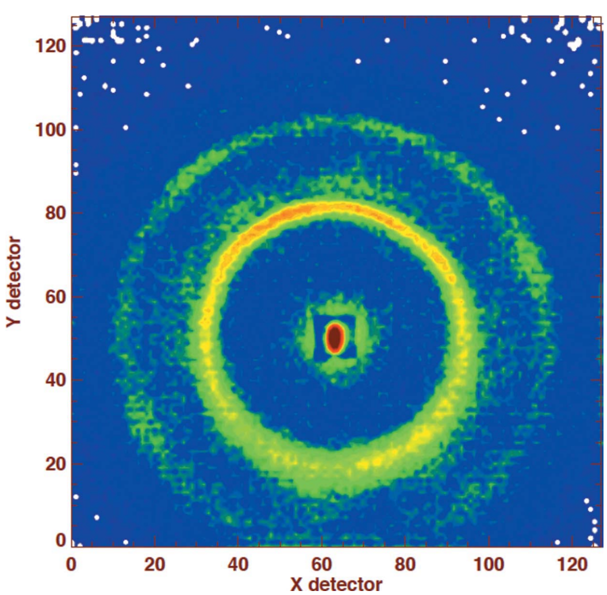

Figure 1
The two-dimensional neutron scattering pattern from opal taken at a wavelength of 10 Å, showing the variation in the resolution of the 111 peak. The weak second diffraction peak at a scattering vector that is $(8/3)^{1/2} \simeq 1.61$ times that of the first-order peak is consistent with a system of close-packed lattice of noncrystalline silica spheres (Sosnowska & Shiojiri, 1999). (The incident beam without the sample is superimposed on the beam stop.)

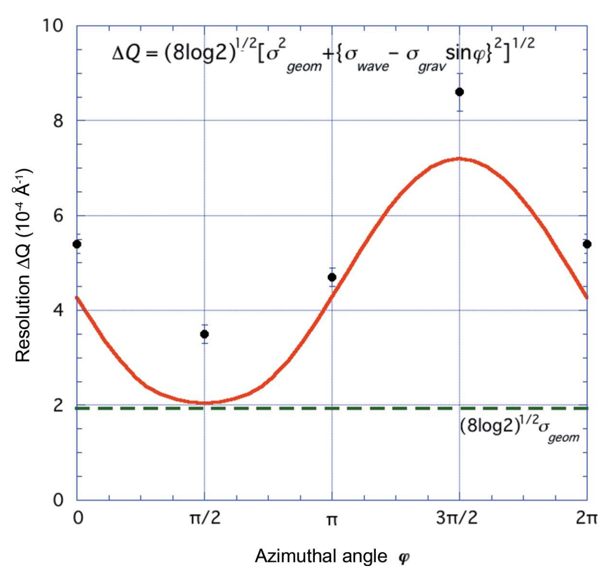

Figure 2
The variation of the FWHM of the diffraction peak for opal using $\lambda = 10$ Å neutrons as a function of azimuthal angle φ. The line is the calculation and the points are the measured data. Both are averaged over 20°. The statistical error bars correspond to one standard deviation.

lution.) Fig. 2 shows these widths as a function of azimuth. These results suggest that there is some extra width of approximately 3×10^{-4} Å^{-1} caused by polydispersity.

4. Conclusions

We have calculated the gravitational distortion of the Debye–Scherrer ring in the scattering pattern of opal and shown reasonable agreement with experimental data. This is the first time that the theory has been compared with measurements. We note the difference between the result given by equation (6) and that given earlier for a single-crystal measurement at low scattering vectors (Mildner *et al.*, 2011). For the latter (what we may call a vector **Q** measurement) the two contributions to the resolution that depend on wavelength spread are both vectors. They need to be summed as vectors, so that the variance along the direction of the major axis of the diffraction ellipse at $\mathbf{Q}_0$ is given by

$$(\sigma_{Q_\parallel})^2 = \sigma^2_{\rm geom} + \left[\mathbf{Q}_0 - 2A\lambda_0^2(k/L_2)\hat{\mathbf{y}}\right]^2(\sigma_\lambda/\lambda)^2, \qquad (7)$$

where $\hat{\mathbf{y}}$ is the unit vector in the vertical direction, so that $Q_0 \cdot \hat{\mathbf{y}} = |Q_0| \sin\varphi$. While the center of the diffraction pattern is $-A\lambda_0^2$ vertically below the spectrometer axis, the major axes of the diffraction spots intersect at a point $+A\lambda_0^2$ above the origin. For the azimuthally symmetric scattering data that we have discussed here (and may call a scalar Q measurement), the component of the gravitational contribution along the scattering vector is added to the magnitude of Q. Hence the equivalent variance is given by equation (6), with the origin of the scattering vectors at $-A\lambda_0^2$, the beam center corresponding to the mean wavelength. This result may be used to smear the scattering from a model function that would have azimuthal symmetry in the absence of gravity for comparison with experiment.

The authors thank Peter Lindner for the use of the opal data, acknowledge discussions with John Barker and thank Boualem Hammouda for critical reading of the manuscript.

References

Barker, J. G. & Pedersen, J. S. (1995). *J. Appl. Cryst.* **28**, 105–114.
Boothroyd, A. T. (1989). *J. Appl. Cryst.* **22**, 252–255.
Graetsch, H. & Ibel, K. (1997). *Phys. Chem. Miner.* **24**, 102–108.
Lindner, P. & Schweins, R. (2010). *Neutron News*, **21**(2), 15–18.
Mildner, D. F. R., Barker, J. G. & Kline, S. R. (2011). *J. Appl. Cryst.* **44**, 1127–1129.
Mildner, D. F. R. & Carpenter, J. M. (1984). *J. Appl. Cryst.* **17**, 249–256.
Sosnowska, I. M. & Shiojiri, M. J. (1999). *Electron Microsc.* **48**, 681–687.